Supplementary Materials

The multiple transformed ZnO ENPs in the aquatic environment: the mechanisms of formation and ecotoxicological impact

Mikołaj Feculak[1], Susana Loureiro[2], Patrícia V. Silva[2], Fábio Yu Chen[2], Patryk Oleszczuk[3], Magdalena Kończak[4], Izabela Jośko[1],*

[1] Institute of Plant Genetics, Breeding and Biotechnology, Faculty of Agrobioengineering, University of Life Sciences, Lublin, 20-950, Poland.

[2] CESAM- Centre for Environmental and Marine Studies & Department of Biology, University of Aveiro, Aveiro, Portugal.

[3] Department of Radiochemistry and Environmental Chemistry, Institute of Chemical Sciences, Faculty of Chemistry, Maria Curie-Sklodowska University, 3 Maria Curie-Sklodowska Square, 20-031 Lublin, Poland

[4] Institute of Earth and Environmental Sciences, Faculty of Earth Sciences and Spatial Management, Maria Curie-Skłodowska University, Al. Kraśnickie 2d, 20-718, Lublin, Poland

* Correspondence to: Izabela Jośko, Institute of Plant Genetics, Breeding and Biotechnology, Faculty of Agrobioengineering, University of Life Sciences in Lublin, 20–950 Lublin, 13 Akademicka Street, Poland, tel. +48 81 4456675, fax. +48 81 4456031, e–mail: izabela.josko@up.lublin.pl

Number of pages: 4

Number of tables: 0

Number of figures: 4

Materials and methods

Characteristics of Pristine and Transformed ENPs

XRD: X-ray diffraction (XRD) measurements were performed using an Empyrean diffractometer (PANalytical, Netherlands) operating with CuKα radiation (λ = 1.54016 Å) at 60 keV, scanning over a 2θ range of 5° to 95°. Phase identification was carried out by matching the recorded diffraction patterns with entries in the PDF-2 database provided by the International Centre for Diffraction Data (ICDD). To enhance the precision of structural parameters, all diffraction data were subjected to Rietveld refinement. Crystallite sizes were estimated based on the resulting XRD patterns using the Debye–Scherrer formula.[1]:

$$D = \frac{K\lambda}{\beta cos\theta} \quad (1)$$

where D is the crystallite size, K is the Scherrer constant (0.9), λ is the wavelength of the X-rays used (1.54016 Å), β is the Full Width at Half Maximum ($FWHM$, radians), and θ is the peak position (radians).

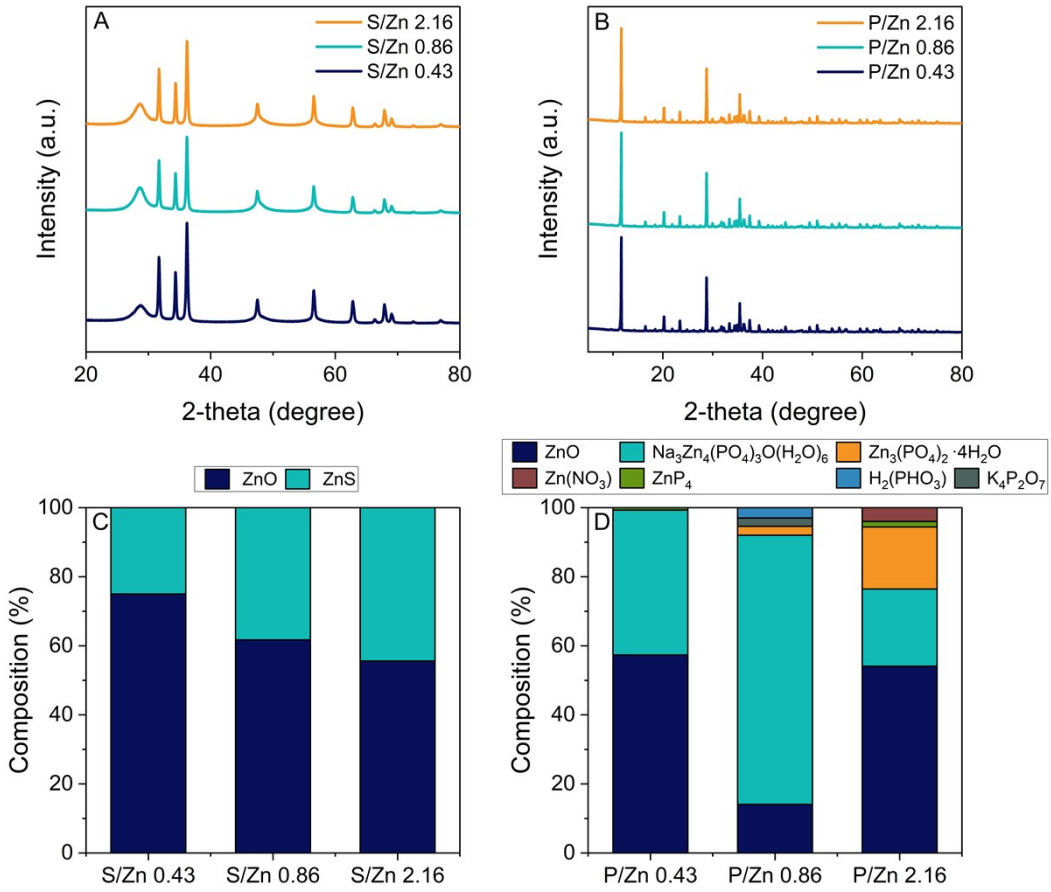

Fig. S1. XRD patterns of sulphidated (**A**) and phosphorylated (**B**) ZnO synthesized at a specific molar ratio are presented, accompanied by their corresponding phase composition analyses (**C, D**).

ICP-OES: For ICP-OES analysis, samples were digested using a mixture of HCl and HNO_3 in a 3:1 volume ratio within Teflon digestion vessels, employing a microwave-assisted digestion system (Milestone ETHOS EASY, Italy) at 180 °C for 15 minutes. An axial viewing configuration was used to enhance detection sensitivity and reduce spectral interferences. The emission wavelengths selected for quantification were 324.754 nm for copper and 213.856 nm for zinc, chosen to ensure high analytical precision and accuracy.

XRF: For XRF analysis, X-rays were generated using a Rh SST-mAX ceramic X-ray tube equipped with a 4 kW anode.

FTIR: To deconvolute overlapping spectral features, second-derivative analysis was employed (Fig. S2A, D), followed by nonlinear regression fitting using Gaussian functions to quantify the contributions of individual secondary structure elements (Fig. S2B, C, E, F). The relative proportion of each structural component (fi) was determined as [2]:

$$f_i = \frac{A_i}{\sum A} \quad (2)$$

where A_i is the area under the corresponding Gaussian peak, and $\sum A$ is the total area of all assigned peaks.

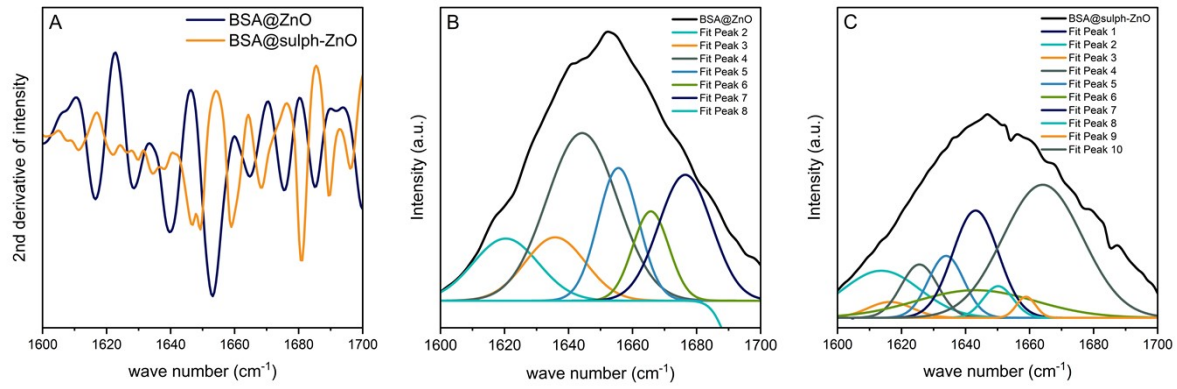

Fig. S2. FTIR spectral analysis of the Amide I band was conducted to assess the secondary structures of proteins adsorbed onto the surfaces of BSA@ZnO and BSA@sulph-ZnO. Second-derivative processing was applied to enhance spectral resolution (**A**), followed by nonlinear Gaussian curve fitting of the Amide I region for BSA@ZnO (**B**), and BSA@sulph-ZnO (**C**), enabling quantitative evaluation of protein secondary structure components.

XPS: To determine the chemical state of the element, the modified Auger parameter was calculated:

$$\alpha = E_K(C_1C_2C_3) + E_B(C_n) \quad (3)$$

where E_K - represents the kinetic energy associated with the most prominent and well-defined $core_1$-$core_2$-$core_3$ (C_1-C_2-C_3) Auger transition (LMM), and E_B - denotes the binding energy corresponding to the most distinct and sharply defined $core_n$ (C_n) ionization peak [3].

Results

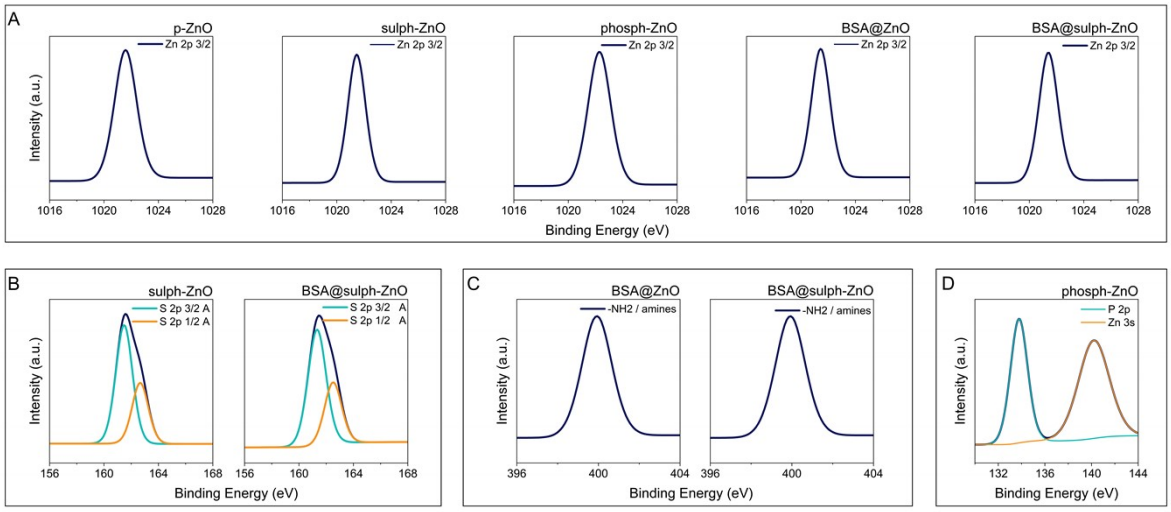

Fig. S3. High-resolution XPS spectra of Zn 2p (**A**), S 2p (**B**), N 1s (**C**), and P 2p (**D**) obtained for p- and trans-ZnO ENPs.

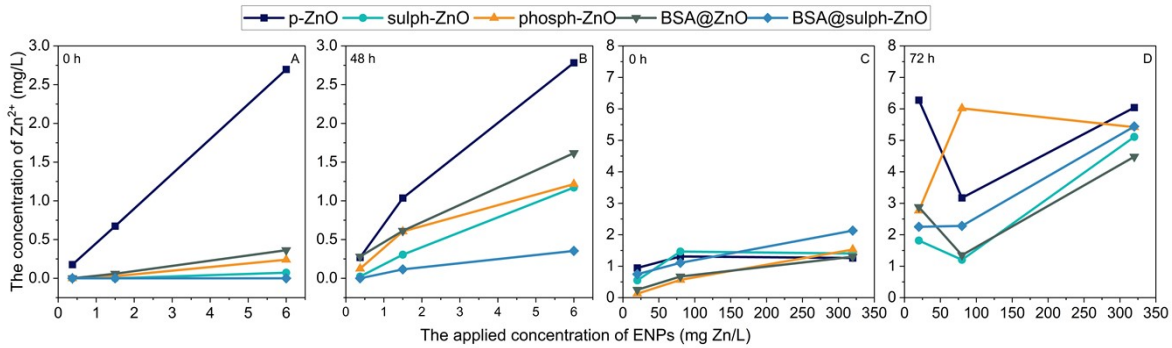

Fig. S4. Concentration of metal ions released from p-ZnO and trans-ZnO ENPs in ASTM solution at 0 h (**A**) and 24 h (**B**), and in MQ water at 0 h (**C**) and 72 h (**D**).

References

1 P. Banerjee and P. K. Jain, Mechanism of sulfidation of small zinc oxide nanoparticles, *RSC Adv.*, 2018, **8**, 34476–34482.

2 H. Yang, S. Yang, J. Kong, A. Dong and S. Yu, Obtaining information about protein secondary structures in aqueous solution using Fourier transform IR spectroscopy, *Nat. Protoc.*, 2015, **10**, 382–396.

3 M. C. Biesinger, L. W. M. Lau, A. R. Gerson and R. St. C. Smart, Resolving surface chemical states in XPS analysis of first row transition metals, oxides and hydroxides: Sc, Ti, V, Cu and Zn, *Appl. Surf. Sci.*, 2010, **257**, 887–898.